Contents lists available at ScienceDirect

Ecological Indicators

Exploring the driving forces of farmland loss under rapidurbanization using binary logistic regression and spatial regression: A case study of Shanghai and Hangzhou Bay

Rui Xiao[a], Yue Liu[a], Xin Huang[a,b,*], Ruixing Shi[a], Weixuan Yu[a], Tao Zhang[b]

[a] School of Remote Sensing and Information Engineering, Wuhan University, Wuhan 430079, China
[b] State Key Laboratory of Information Engineering in Surveying, Mapping and Remote Sensing, Wuhan University, Wuhan 430079, China

ARTICLE INFO

ABSTRACT

The unprecedented accelerating urbanization in China has led to a sharp decline in cultivated land. In this paper, the dynamics of farmland patterns during three periods (1994–2003, 2003–2009, 2009–2015) in the Shanghai and Hangzhou Bay (SHB) area are exhibited by dynamic change models and standard deviation ellipse analysis. Additionally, further detection of the determinants of farmland loss is carried out, through a combination of binary logistic regression and spatial regression models. Seven proximate driving factors are selected: distance to water; distance to coastline; distance to city center; and distance to roads (provincial road, national road, highway, and railway). The results suggest that Shanghai experienced the most drastic changes in farmland during the study periods across the whole city agglomeration, and this impact spatially diffused to its adjacent cities. Meanwhile, the transportation routes, especially for provincial road and national road, are quantitatively verified to be the most prominent determinants with a negative influence. Our research highlights that the serious farmland loss should be addressed in highly urbanized area. Furthermore, there is an urgent need for the government to formulate efficient policies for farmland protection and to curb the spread of this phenomenon in the urban agglomeration.

1. Introduction

Soils are the foundation of our civilization, and they provide us with not only a veneer for the Earth system, but also a common rendezvous point for human activities (Haygarth & Ritz, 2009). In China, almost a quarter of soils are agricultural land (Suet al., 2012), which guarantees a long-lasting food supply and stable ecosystem service for human society (Osawa et al., 2016). However, the conflict of farmland with accelerating urbanization and industrialization is gradually becoming a subject of controversy in modern China (Huang et al., 2005). Typically, the most fertile and productive land is lost to urbanization, directly resulting in the decrease of farmland (Zhou et al., 2017). As more farmland is converted to other use, the question arises as to whether this trend represents a systematic reduction in our ability to produce food by placing our infrastructure on the valuable soil resources (Zhang et al., 2007).

Given the composite application of remote sensing (RS), geographical information systems (GIS), and regression analysis methods, considerable efforts have been made to survey the spatial pattern dynamics of agricultural land (Tan et al., 2005) and to explore the specific driving forces under rapid urbanization (Zhang et al., 2013). Su et al. (2014a,b,c) identified the interrelationship between urbanization and agricultural landscape patterns at an ecoregional scale by utilizing a series of urbanization indicators; Zhou and Li (2017) developed an evaluation framework for urban agricultural land-use efficiency to provide the mechanism of spatio-temporal changes in the Xi'an metropolitan zone; Hu and Zhang (2013) introduced a post-classification change detection technique to assess the impacts of urbanization on seasonal land use and land cover (LULC) changes. Some other studies (Durina et al., 2013; Chaudhuri and Mishra, 2016) have also hypothesized that land-use conversion could be incorporated into national and local land-use planning policies, particularly in coastal zones, in order to achieve sustainable farmland regulation and management.

Although a myriad of evidence of the threat to farmland has been

---

* Corresponding author at: School of Remote Sensing and Information Engineering, Wuhan University, Wuhan 430079, China and State Key Laboratory of Information Engineering in Surveying, Mapping and Remote Sensing, Wuhan University, Wuhan 430079, China.
E-mail addresses: rxiao@whu.edu.cn (R. Xiao), yliu_rs@whu.edu.cn (Y. Liu), xhuang@whu.edu.cn (X. Huang), ruixingshi@whu.edu.cn (R. Shi), wxyu@whu.edu.cn (W. Yu).

presented, few studies have quantitatively determined the specific driving forces under rapid urbanization, especially for large urban agglomerations. Generally speaking, the megacity within a city group radiates and promotes the effects of urbanization to its adjacent small- and medium-sized cities and towns (Chace and Walsh, 2006). Among the most alarming consequences of urban sprawl onto the surrounding areas are the steady and irreversible shrinkage of farmland and the conflicts arising from the mixed functions performed by these areas (Kacprzak and Maćkiewicz, 2013). The complexity of the driving forces is closely related to the properties of the study area, and studying the same region at different scales can identify different driving forces (Yan and Cai, 2015). The neighborhood, physical factors, proximity, and socio-economic factors are the universally recognized determinants of land transition (Liao and Wei, 2014). In this paper, we focus on quantifying the relationship between the proximate driving factors and cultivated land loss under urbanization in a coastal urban agglomeration, using a novel method of combining spatial regression and binary logistic regression models. The findings will help to reveal the current farmland loss resulting from rapid urbanization. More than this, our findings will also provide a scientific basis for government to initiate agricultural protection policies, carry out urban planning, and optimize the land regulations of coastal cities.

To be specific, we attempt to: 1) evaluate the spatial pattern and temporal dynamics of cultivated land at an administrative scale over three periods (1994–2003, 2003–2009, 2009–2015) across the Shanghai and Hangzhou Bay (SHB) area; 2) identify the potential proximate determinants of farmland conversion, considering the spatial aggregation and diffusion in the coastal urban agglomeration; 3) provide an innovative way to combine multiple regression methods in driving force analysis; and 4) assist the relevant departments to translate the macro farmland policy in China into local land-use practices.

2. Study area and materials

2.1. Study area

As shown in Fig. 1(a), the SHB area is located in the coastal part of southeastern China, extending from 28.9°N to 31.2°N and from 118.3°E to 122.3°E. Along with the urban agglomeration along the Yangtze River, the SHB area forms the Yangtze River Delta megaregion. In this area, there is one provincial capital (Hangzhou), one province-level municipality (Shanghai), and four metropolises (Huzhou, Shaoxing, Ningbo, and Jiaxing). Close business contact and frequent population flow take place between these cities.

In addition, due to the proximity of the geographical location, the climatic conditions and soil environments of this urban agglomeration are very similar. The SHB area enjoys a humid subtropical climate. Its average temperature in January is generally above 0 °C, and the temperature in July is generally around 25 °C. The average annual precipitation amounts to 1460 mm. Under the combined effects of rivers, rainfall and climate, the soil in the Yangtze River Delta is moist and full of nutrients, which give the productivity and thereby attracting a great number of people to settle down and develop here. According to the statistics, the population of the SHB area increased from 20.52 million to 47.81 million during the 20 years of 1994–2015. From Fig. 1(b), it can be seen that a large area of plains is found in the northeast and the central part of the SHB area, which provides suitable topographic conditions for crops to grow. The entire SHB area covers an area of 50,764 km², and in 2015, the total cultivated land area amounted to 19.84% of it (Zhejiang Statistical Yearbook, 2016; Shanghai Statistical Yearbook, 2016).

The SHB area is equipped with three major natural harbors (Shanghai port, Ningbo port, Yangshan port), which provide convenient transportation and business conditions (Fig. 1(c)). Driven by these economic benefits, the SHB area has mushroomed to become one of the most urbanized regions in the world. Such rapid urbanization has had a

significant impact on the soil, and especially the cultivated land. Therefore, we chose the SHB area as a typical example to investigate the determinants of farmland loss in the process of urbanization.

2.2. Land-use data acquisition and processing

The data for the cultivated land in Hangzhou Bay (1995, 2000, 2005, 2010) and the city of Shanghai (1995, 2000, 2005, 2010) were obtained from Xiao et al. (2013a,b) and Su et al. (2014a,b,c), respectively. On this basis, we downloaded Landsat Thematic Mapper (TM) remote sensing images at a 30-m resolution (1994, 2003, 2009, 2015) from http://glovis.usgs.gov/. Before the interpretation, all the images were geometrically corrected and false-color composited. To allow us to compare these remote sensing images, we extracted the cultivated land data by visual interpretation in the corresponding year. Considering the coarse resolution and the presence of mixed spectral phenomena, farmland was not subdivided into specific categories (e.g., red soil, paddy soil, etc.) in the process of classification. To check the result of the interpretation, we linked Google Maps with ArcGIS 10.1 software and selected 500 random points on the map within the scope of the study area. The accuracy reached 78.2% for 1994, 81.1% for 2003, 83.4% for 2009, and 85.2% for 2015, respectively, satisfying the accuracy requirements. After obtaining the data of farmland distribution in each year, we further processed it and got the change maps of farmland between 1994 and 2003, 2003–2009, 2009–2015, which are shown in Fig. 2.

2.3. Selection of potential driving factors

A transition in land use is not a stationary pattern, nor is it deterministic (Lambin and Meyfroidt, 2010). Farmland loss can be caused by the negative socio-ecological feedback that arises from a set of structural or behavioral factors (Tayyebi and Pijanowski, 2014). In this study, we referred to previous studies (Shu et al., 2014; Li et al., 2013), which proposed that among the potential variables, accessibility is the most important one. The spatial characteristics of the surface features and the availability of the data were also taken into consideration. Thus, in this study, we finally focused on exploring the role of the different proximate driving factors.

More specifically, proximity determinants include the distance to city centers, rivers and lakes, transportation routes, or some special objects (Xiao et al., 2015). In this study, the administrative center of each city was extracted as a representative of the city center. The early urbanization demonstrated an expansion pattern from the city centers into the rural areas (Wu et al., 2015). The distance to city center (D_{cc}) indicates the degree of human aggregation. Located near the Yangtze River Basin, the SHB area features an extensive water system, which plays an important role in the agricultural production activities and urban development. Thus, the distance to water (D_{wt}) was also included in the analysis. Land use along the major roads has undergone a substantial level of change from agricultural farm land to residential and commercial uses (Oruonye, 2014). We therefore selected four traffic variables for complete exploration: distance to provincial road (D_{pr}), distance to national road (D_{nr}), distance to highway (D_{hw}), and distance to railway (D_{rw}). Furthermore, as a coastal urban agglomeration, the coastlines affect the LULC and human societies significantly (Wu et al., 2018), so the distance to coastline (D_{cl}) was also taken into account. The spatial patterns of these determinants in the study area are shown in Fig. 3 in detail.

All the digital geographic data were obtained from the national basic geographic data sets (1:4000,000 scale). In particular, the coastline data were downloaded from https://shoreline.noaa.gov/. Using these data sources, we calculated the distance to each factor using the NEAR module in ArcGIS 10.1. What should be mentioned is that our research was carried out on a large-scale basis, so census-based variables such as population density and gross domestic product (GDP)
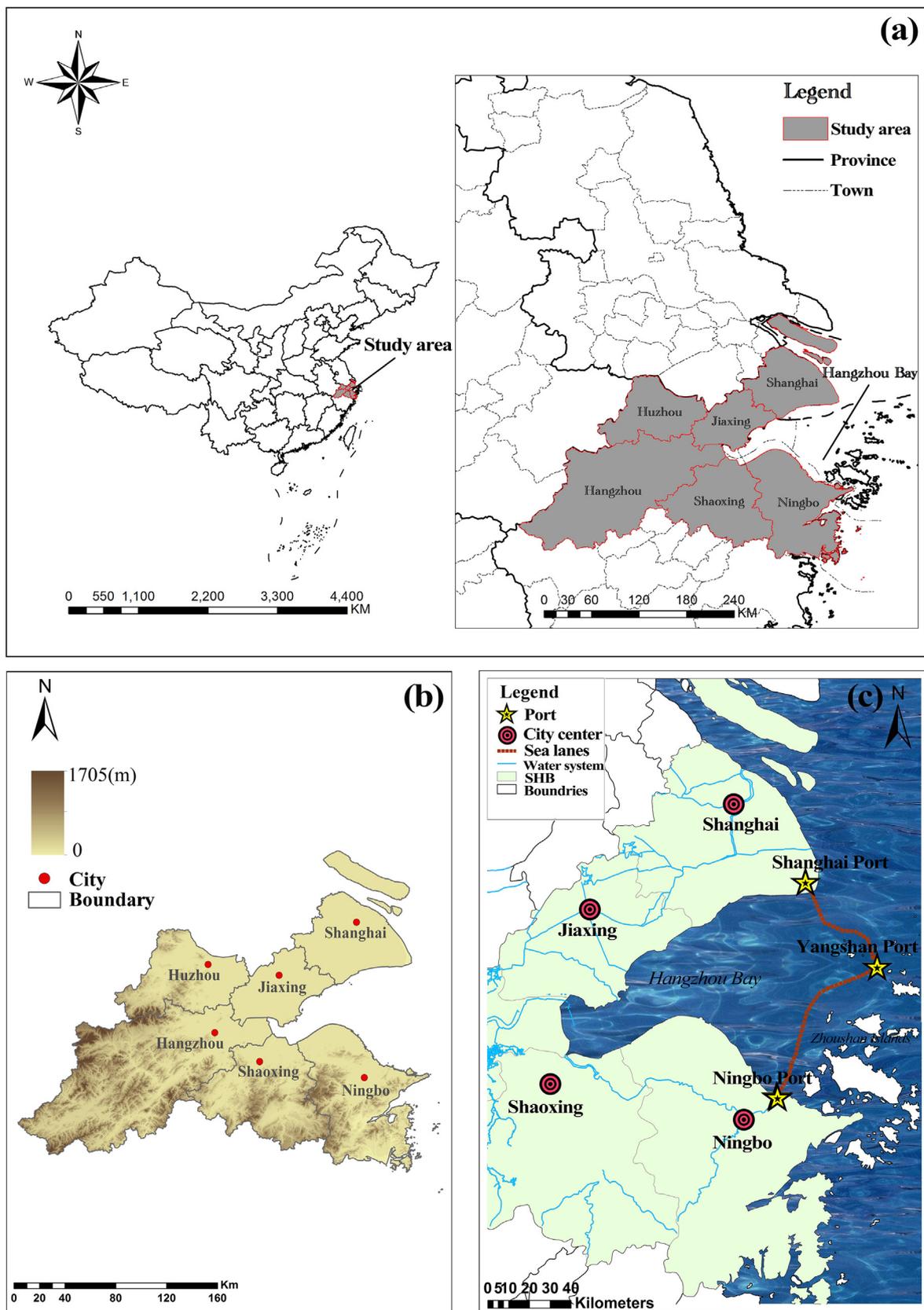
Fig. 1. The study area of Shanghai and Hangzhou Bay (SHB). (a) The location of the urban agglomeration around the SHB area. (b) The elevation. (c) The major natural harbors in the SHB area.
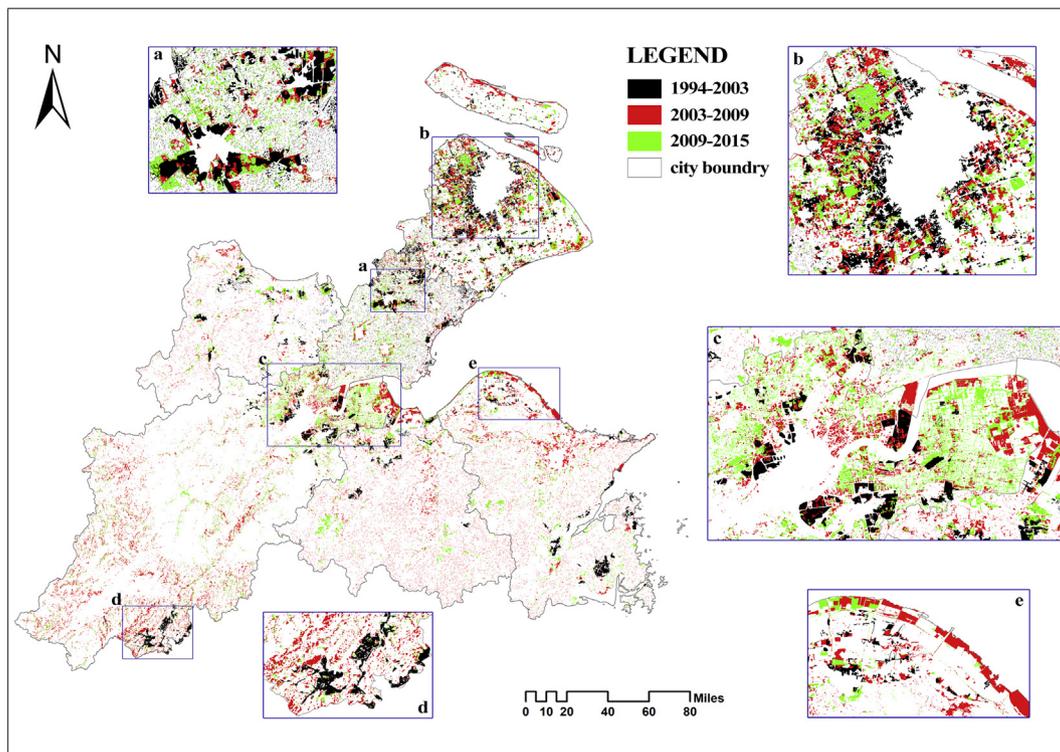
Fig. 2. The farmland changes of the Shanghai and Hangzhou Bay (SHB) area in 1994–2003, 2003–2009, and 2009–2015. a–e highlights some areas with intense changes.

were not incorporated.

3. Methodology

3.1. Cultivated land change model

Changes in river systems, urban centers, coastlines, and road construction can transform the farmland distribution and result in the unsustainable development of regional agriculture. The introduction of LULC change models are of great help to the comprehensive evaluation of such changes. In this study, the cultivated land-use dynamics index (CLUDI) was employed for the analysis of the farmland patterns, expressed as shown in Eq. (1). Considering the different time spans of T1 (1994–2003), T2 (2003–2009), and T3 (2009–2015), the CLUDI normalizes the value of T, so as to better explore the quantity change of a single land-use type in a certain period.

$$CLUDI = \frac{U_a - U_b}{U_a} \times \frac{1}{T} \times 100\% \tag{1}$$
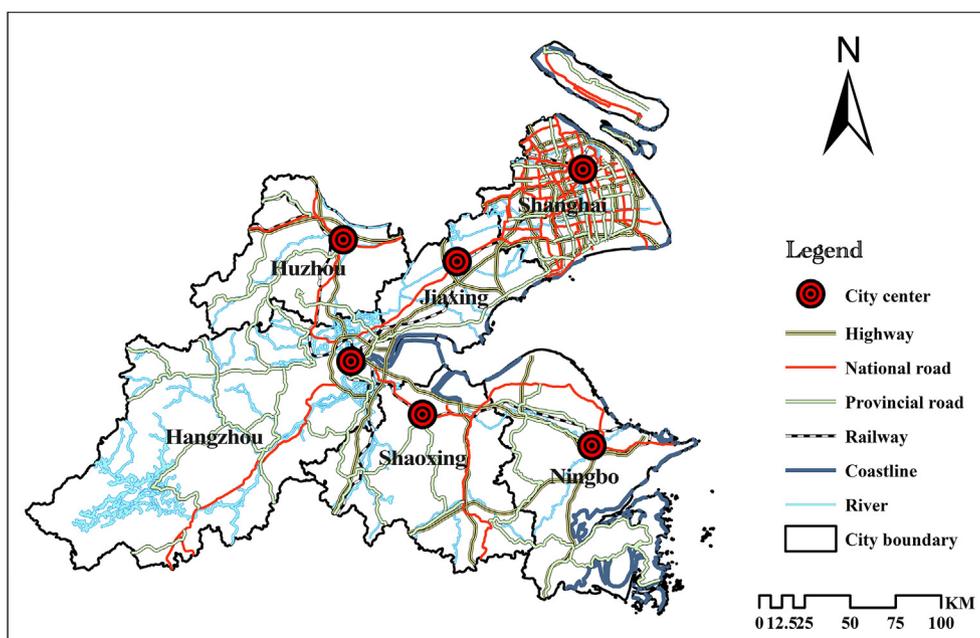
Fig. 3. The spatial patterns of selected potential determinants (water, coastline, city center, provincial road, national road, highway, and railway) in the SHB cities.

Table 1
Results of the CLUDI and RDI models.

	T1	T2	T3	T1		T2		T3	
	CLUDI			RDI	Rank	RDI	Rank	RDI	Rank
Hangzhou	−0.010	−0.053	−0.028	0.499	3	0.445	1	0.214	2
Shanghai	−0.007	−0.018	−0.022	0.542	2	0.243	2	0.343	1
Huzhou	−0.004	−0.007	−0.010	0.181	5	0.05	5	0.1	4
Shaoxing	−0.001	−0.013	−0.011	0.072	6	0.127	3	0.123	3
Ningbo	0.015	−0.004	−0.010	−0.678	1	0.042	6	0.123	3
Jiaxing	−0.009	−0.013	−0.011	0.384	4	0.092	4	0.098	5
SHB	−0.003	−0.018	−0.015	1		1		1	

Abbreviations: cultivated land-use dynamics index (CLUDI); regional difference index (RDI); Shanghai and Hangzhou Bay (SHB). T1: 1994–2003, T2: 2003–2009, T3: 2009–2015. The underlined numbers are regions which showed greater change.
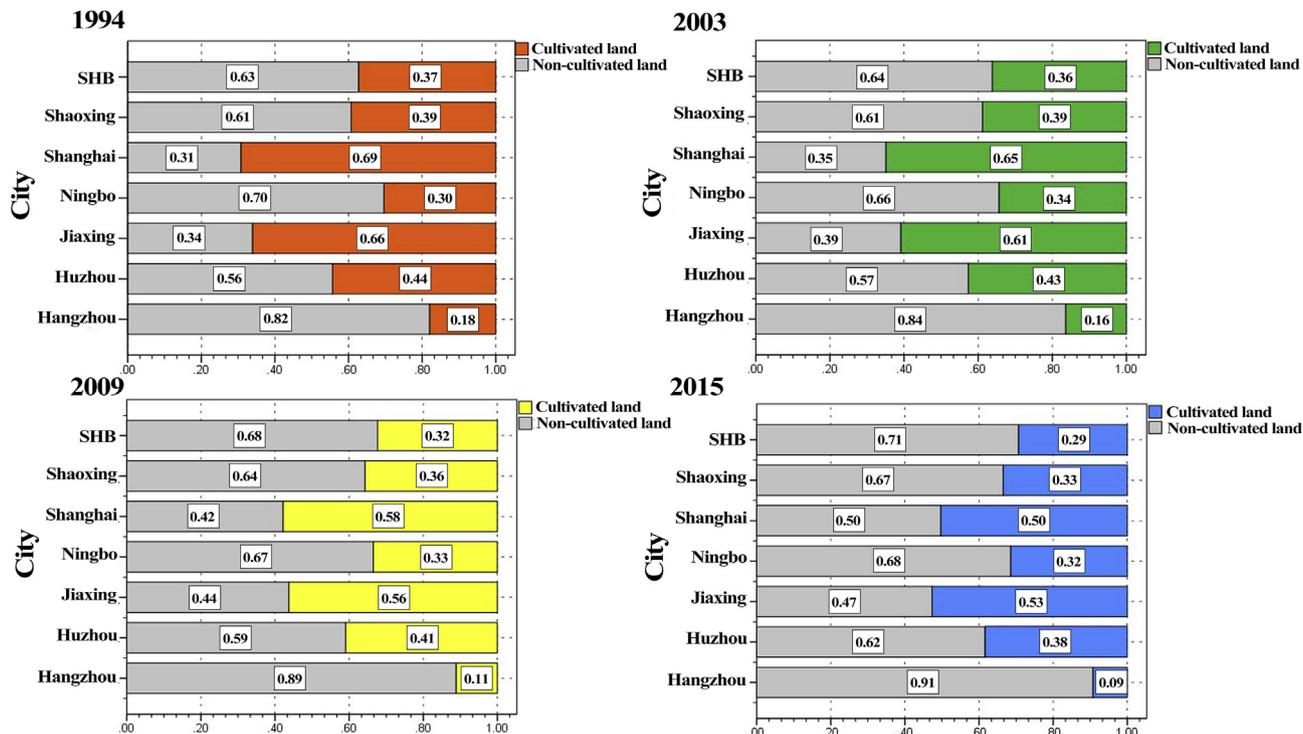
Fig. 4. The proportion of cultivated land and non-cultivated land in 1994, 2003, 2009, and 2015.

where *CLUDI* represents the dynamic degree of cultivated land use in the study area; U_a and U_b are the total area of cultivated land at the beginning and the end of the study period, respectively; T denotes the years of a study period, and if the period of T is set to year, the value of *CLUDI* is the annual percentage change rate of the cultivated land.

In addition, the regional difference index (RDI) was also applied, to reflect the regional synthetic differences of LULC change. If the relative change rate of farmland in a certain city is determined as RDI > 1, it indicates that the farmland change in this region is larger than that of the whole region. The expression of this model is represented as shown in Eq. (2):

$$RDI = \left[\frac{K_b}{K_a} \right] / \left[\frac{C_b}{C_a} \right] \tag{2}$$

where *RDI* is the RDI of cultivated land-use change; K_a and K_b represent the area of farmland in a particular city at the beginning and the end of the study period, respectively; and C_a and C_b represent the area of farmland across the whole SHB at the beginning and the end of the study period, respectively.

3.2. Standard deviation ellipse analysis

A common way to measure the trend of a set of points or areas is to calculate the standard distance separately in the x- and y-directions. These two measures define the axes of an ellipse encompassing the distribution of features. The ellipse is referred to as the standard deviational ellipse (SDE), since the method calculates the standard deviation of the x-coordinates and y-coordinates from the mean center to define the axes of the ellipse (Gong, 2002). In this study, we applied the mean center of cultivated land within a certain city as the center of the SDE, and its formula is shown in Eq. (3). Recognizing the spatio-temporal distribution of cultivated land using the ellipse allows us to understand the spatial characteristics of the geographic features of central tendency, directional trends, and dispersion. The formula for structuring the SDE is denoted as shown in Eq. (4) (Lefever, 1926).

$$\overline{X} = \frac{\sum_{i=1}^{n} x_i}{n}, \quad \overline{Y} = \frac{\sum_{i=1}^{n} y_i}{n} \tag{3}$$

where x_i and y_i are the coordinates for feature *i*, and *n* is equal to the total number of features.
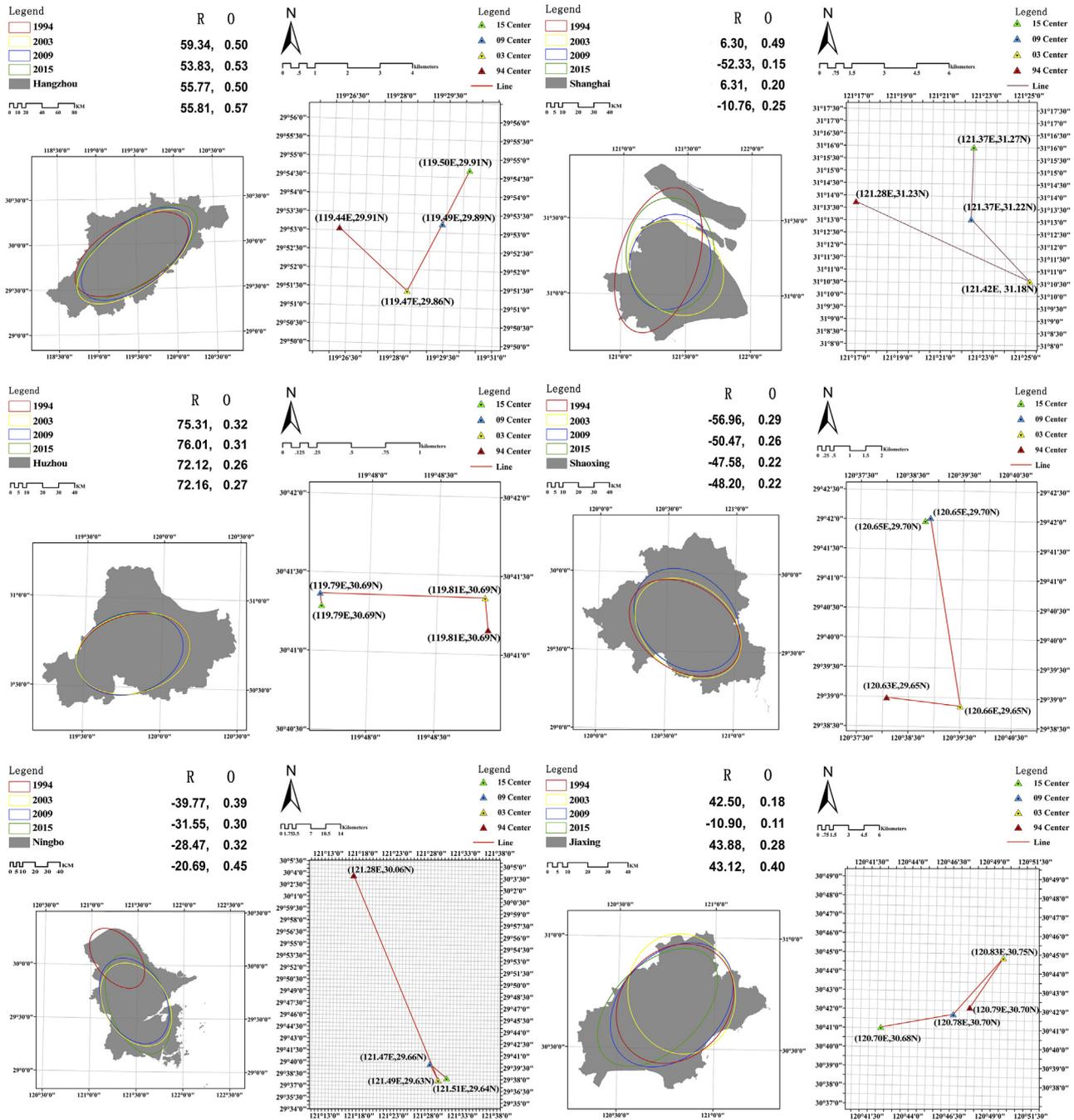
Fig. 5. Distribution of cultivated land in the six cities in 1994, 2003, 2009, and 2015. The standard deviation ellipse is shown in the left column and its weighted mean center in the right column (the rotation angle of SDE(R), the oblateness of SDE(O)).

$$SDE_x = \sqrt{\frac{\sum_{i=1}^{n}(x_i - \overline{X})^2}{n}}, \quad SDE_y = \sqrt{\frac{\sum_{i=1}^{n}(y_i - \overline{Y})^2}{n}} \tag{4}$$

where x_i and y_i are the coordinates for feature i, $\{\overline{X}, \overline{Y}\}$ represents the mean center for the features, and n is equal to the total number of features.

In detail, the position of the ellipse center is presumed to be the most representative single position of all locations in the area occupied by the cultivated land, and its change reflects the transfer of the mean center of land gravity (Wang et al., 2015). The angle θ of a long half axis deviating clockwise from the y-coordinates is deemed to be the rotation angle of the SDE, from which the orientation of the land distribution can be signified quantitatively by Eq. (5). Another indicator of the SDE is

oblateness, which is calculated to describe the flattening degree, using the expression of Eq. (6). In particular, the lower the value, the more obviously an ellipse tends to be a circle.

$$\tan\theta = \frac{A+B}{C}$$

$$A = \left(\sum_{i=1}^{n}\tilde{x}_i^2 - \sum_{i=1}^{n}\tilde{y}_i^2\right)$$

$$B = \sqrt{\left(\sum_{i=1}^{n}\tilde{x}_i^2 - \sum_{i=1}^{n}\tilde{y}_i^2\right)^2 + 4\left(\sum_{i=1}^{n}\tilde{x}_i\tilde{y}_i\right)^2}$$

$$C = 2\sum_{i=1}^{n}\tilde{x}_i\tilde{y}_i \tag{5}$$

Table 2
Summary of the BLR models.

Variable	Period	Hangzhou	Shanghai	Huzhou	Shaoxing	Ningbo	Jiaxing
D_{wt}	T1	0.140**	0.020**		−0.108**	0.115**	0.037*
	T2	−0.017*	0.019**				
	T3		0.030**	−0.059**	−0.033*	0.050**	−0.062**
D_{cl}	T1	−0.068**				−0.233**	−0.127**
	T2	−0.054**	0.009**			−0.027**	−0.109**
	T3	0.010*			−0.036**	0.029**	
D_{cc}	T1		−0.047**		−0.111**	−0.088**	−0.025**
	T2		−0.044**		−0.027**	−0.009*	0.024**
	T3		−0.066**		0.041**		
D_{pr}	T1	−0.058**	−0.099**	−0.146**		−0.053**	0.175**
	T2	−0.028**	−0.067**		0.035**		0.149**
	T3		−0.144**	−0.042*	−0.063**		
D_{nr}	T1	−0.116**	−0.233**	−0.173**		−0.064**	0.051**
	T2	−0.013**			0.018**		0.037*
	T3	−0.006*	−0.153**	−0.041*	−0.017*		
D_{hw}	T1	0.143**			0.082**	−0.104**	−0.037**
	T2	0.079**	0.017**	0.101**		0.020**	−0.074**
	T3		−0.054**	−0.068**	−0.067**	−0.053**	
D_{rw}	T1	−0.086**	−0.039**	0.147**		0.103**	
	T2			−0.042*	0.022**		
	T3		0.026**	0.040*	−0.029**		−0.083**
Constant	T1	−0.453*	0.555**	−2.159**	−1.013**	0.954*	−2.293**
	T2	−0.779**	−0.485**	−2.651**	−2.211**	−0.915**	−3.197**
	T3	−0.420**	0.633**	−2.090**	−0.988**	−3.242**	−1.418**

	Hangzhou			Shanghai			Huzhou			Shaoxing			Ningbo			Jiaxing		
Period	T1	T2	T3	T1	T2	T3	T1	T2	T3	T1	T2	T3	T1	T2	T3	T1	T2	T3
AUC ROC	0.82	0.68	0.55	0.77	0.64	0.76	0.70	0.66	0.67	0.87	0.61	0.70	0.86	0.62	0.59	0.69	0.59	0.67
Adjusted R^2	0.28	0.12	0.01	0.20	0.05	0.19	0.07	0.05	0.03	0.24	0.04	0.07	0.29	0.04	0.02	0.08	0.03	0.07

Abbreviations: distance to water (D_{wt}), distance to coastline (D_{cl}), distance to city center (D_{cc}), distance to provincial road (D_{pr}), distance to national road (D_{nr}), distance to highway (D_{hw}), distance to railway (D_{rw}), area under the receiver operating characteristic curve (AUC ROC). T1: 1994–2003, T2: 2003–2009, T3: 2009–2015.

 * $p < 0.05$.
 ** $p < 0.01$.

where $\widetilde{x}_i$ and $\widetilde{y}_i$ are the deviations of the *xy*-coordinates from the mean center.

$$O = \frac{a-b}{a} \tag{6}$$

where O is the oblateness of the SDE; and *a*, *b* signify the minor axis semidiameter and major axis semidiameter, respectively.

In the recent studies, the SDE has been commonly adopted to map the distributional trend for a set of specific behaviors, in order to identify the relationship between particular physical features (Kent and Leitner, 2007) or to plot ellipses for a disease outbreak over time so as to establish the spreading model (Eryando et al., 2012), and so forth.

3.3. Binary logistic regression

Binary logistic regression (BLR) is a statistical method commonly applied in geographic information analysis (Menard, 2012a). The goal of BLR is to explore the relationship between a dependent variable and two independent elements with regression models (Lee, 2005). In this study, we established one regression model for each period. Cultivated land change (Y) was considered as the binary dependent variable, and seven selected potential driving forces (D_{wt}, D_{cl}, D_{cc}, D_{pr}, D_{nr}, D_{hw}, D_{rw}) were chosen as the independent variables. If the land converted from cultivated land to other types of LULC, we considered that change occurred and set Y = 1; otherwise, we set Y = 0. Before the regression, there was a need for all the explanatory variables to be standardized and normalized. Given that there are *m* determinants, i.e., $x_i (i = 1, 2, ..., m)$, the overall probability of Y = 1 is P. The BLR model is shown below.

$$P(Y = 1|x_1, x_2, ..., x_m) = \frac{e^{(\beta_0 + \sum \beta_i x_i)}}{1 + e^{(\beta_0 + \sum \beta_i x_i)}}$$

$$\text{logit} P(Y = 1|x_1, x_2, ..., x_m) = \ln\left(\frac{P}{1-P}\right) = \beta_0 + \beta_1 x_1 + ... + \beta_m x_m \tag{7}$$

where β_0 is a constant, and the parameters β_i ($i = 1, 2, ..., m$) are the coefficients of each independent variable to be estimated, which can reveal the possible impact of each independent variable exerted on the dependent variable (Menard, 2012b). In detail, if the dependent variable (Y) is proportional to a factor, we consider that Y is more likely to be 1 under the influence of this factor, which means that the possibility of transformation is greater. The adjusted R^2 can be used in testing the interpretability of logistic regression results (Li et al., 2013). An adjusted $R^2 > 0.2$ denotes a relatively good fit for the model (Shu et al., 2014). In addition, the area under the relative (or receiver) operating characteristics (ROC) curves (AUC-area under curve) was also used as a summary measure to examine the quality of the forecasts with a higher or lower possibility of farmland change (Mason and Graham, 2002). It is testified that when the forecast system is accurate, the AUC values will exceed 0.5 (Pazúr et al., 2014). All of the calculations were undertaken in SPSS 19.0 software.

3.4. Spatial regression

If there is spatial heterogeneity between samples, the spatial regression model should be used to avoid the estimation error (Jiang and Ji, 2011). Therefore, we used spatial regression to investigate the spatial heteroskedasticity and spatial dependence of the error terms for the

Table 3
Determination coefficients of the spatial regression between areas of cultivated land and potential driving forces at the municipal level during the three temporal intervals.

City	Spatial regression model		Adjusted R^2
Hangzhou	T1	$Y^a = (-32.38^{**} \times D_{nr} + 39.10^{*} \times D_{rw}) + 0.99^{**} \times WY + 655564^{**}$	0.755
	T2	$Y^a = (-41.31^{**} \times D_{cl} + 28.54^{**} \times D_{cc}) + 1.00^{**} \times WY$	0.362
	T3	$Y^a = (-2.96^{**} \times D_{cl}) + 0.99^{**} \times WY + 65844.1^{**}$	0.805
Shanghai	T1	$Y^a = (-3.37^{**} \times D_{wt} - 3.65^{**} \times D_{cc} - 30.71^{*} \times D_{nr} - 15.77^{**} \times D_{rw}) + 0.99^{**} \times WY + 644375^{**}$	0.931
	T2	$Y^a = (-22.85^{**} \times D_{pr}) + 0.99^{**} \times WY$	0.957
	T3	$Y^a = (-36.89^{**} \times D_{pr} - 37.84^{**} \times D_{nr} - 11.04^{**} \times D_{hw} + 7.62^{*} \times D_{rw}) + 1.00^{**} \times WY$	0.302
Huzhou	T1	$Y^a = (-19.14^{**} \times D_{wt} - 21.60^{**} \times D_{pr} + 14.72^{**} \times D_{rw}) + 0.97^{**} \times WY + 240868^{**}$	0.406
	T2	$Y^b = (3.84^{*} \times D_{nr}) + 0.99^{**} \times \lambda$	0.491
	T3	$Y^a = (-12.74^{**} \times D_{wt} + 5.64^{**} \times D_{cc} - 6.47^{*} \times D_{hw}) + 0.99^{**} \times WY + 97635.6^{*}$	0.933
Shaoxing	T1	$Y^b = (2.66^{*} \times D_{wt} + 2.80^{*} \times D_{nr} - 5.99^{**} \times D_{hw}) + 0.99^{**} \times \lambda + 1.12 \times 10^{6*}$	0.995
	T2	$Y^a = (-6.92^{**} \times D_{cl} + 4.58^{*} \times D_{pr} + 7.75^{**} \times D_{nr} + 6.72^{**} \times D_{rw}) + 0.99^{**} \times WY$	0.348
	T3	$Y^a = (-8.74^{*} \times D_{wt} - 8.55^{*} \times D_{pr} - 7.90^{**} \times D_{nr} - 6.98^{**} \times D_{rw}) + 1.00^{**} \times WY + 320442^{**}$	0.801
Ningbo	T1	$Y^a = (49.33^{**} \times D_{wt} - 116.15^{**} \times D_{cl} - 32.15^{**} \times D_{cc} - 75.78^{**} \times D_{pr} - 53.48^{*} \times D_{nr} - 62.23^{**} \times D_{hw} + 57.03^{*} \times D_{rw}) + 1.00^{**} \times WY + 2.38 \times 10^{6**}$	0.377
	T2	$Y^a = (-7.77^{**} \times D_{cl} - 7.51^{**} \times D_{pr} - 10.30^{**} \times D_{nr} + 7.99^{*} \times D_{rw}) + 1.00^{**} \times WY + 395117^{**}$	0.350
	T3	$Y^a = (-3.33^{*} \times D_{nr} - 3.76^{*} \times D_{hw}) + 1.00^{**} \times WY + 86328.2^{**}$	0.928
Jiaxing	T1	$Y^a = (-23.92^{*} \times D_{wt} - 35.38^{*} \times D_{cl} + 34.87^{*} \times D_{pr}) + 0.99^{**} \times WY + 488299^{**}$	0.872
	T2	$Y^b = (-4.91^{**} \times D_{cc} - 7.09^{**} \times D_{pr} - 13.89^{**} \times D_{nr} + 7.51^{**} \times D_{hw} + 10.47^{**} \times D_{rw}) + 5.50^{**} \times \lambda + 358161^{**}$	0.568
	T3	$Y^a = (-6.31^{*} \times D_{wt} - 9.09^{**} \times D_{nr} - 5.95^{*} \times D_{hw}) + 0.99^{**} \times WY$	0.885

Abbreviations: distance to water (D_{wt}), distance to coastline (D_{cl}), distance to city center (D_{cc}), distance to provincial road (D_{pr}), distance to national road (D_{nr}), distance to highway (D_{hw}), distance to railway (D_{rw}), area under the receiver operating characteristic curve (AUC ROC). T1: 1994–2003, T2: 2003–2009, T3: 2009–2015.
[*] $p < 0.05$.
[**] $p < 0.01$.
[a] Spatial lag models.
[b] Spatial error models.

driving force analysis of changing farmland patterns (Fang et al., 2016). The spatial regression model consisted of a spatial lag model (SLM) and spatial error model (SEM). The former model was applicable when the farmland in the region was affected by its neighboring regions, while the latter model was advantageous in detecting the spatially random error terms (Xiao et al., 2013a,b).

The formulation of the SLM is described as shown in Eq. (8) (Anselin, 1995):

$$y = \rho W_y + X\beta + \varepsilon \qquad (8)$$

where y represents the area of each changing farmland feature; W_y is a spatially lagged dependent variable for the weight matrix W; X is a matrix of independent observations; ε is a vector of error terms; and ρ and β are coefficient vectors.

Equations characterizing the SEM are shown in Eqs. (9) and (10) (Anselin, 1995):

$$y = X\beta + \varepsilon \qquad (9)$$

$$\varepsilon = \lambda W_\varepsilon + \mu \qquad (10)$$

where y is a vector containing the area of each changing farmland feature; X is a matrix of independent observations; W_ε is the spatial weight matrix; ε is a vector of the spatial error terms; and β and λ are coefficient vectors.

For these two models, if the value of β tends to be positive, then the farther the distance to the factor, the greater the impact will be; otherwise, it assumes an opposite relationship. All the spatial regression models were computed in GeoDa 0.9.5-i (Beta) software, and the independent variables were entered into the regression in a stepwise way to avoid the potential multicollinearity among factors (Su et al., 2013).

4. Results

4.1. Dynamic features of cultivated land change

Table 1 shows the results of the CLUDI and RDI models in the SHB cities during the three different periods. For the CLUDI, it displays a negative growth in all cities and periods, except for the city of Ningbo in T1, indicating that majority of the cultivated land in the SHB area was decreasing during the study period. Among these cities, the change speed of Shanghai and Huzhou became faster and faster, while in other cities, the change speed first presented an increasing trend and then decreased, which implies that Shanghai and Huzhou were experiencing rapid urbanization while the other cities had entered a period of stabilization. As far as the whole of the SHB area, the gross area of cultivated land declined most significantly in T2 (2003–2009), which was six times that of the change rate in T1 (1994–2003) and 1.2 times that of T3 (2009–2015), revealing the divergence over time. Moreover, significant differences happened across space, according to the value of the RDI. From the comprehensive ranking of T1, T2, and T3, Shanghai was found to be the region which went through the most drastic transformation of cultivated land, followed by Hangzhou. Additionally, in spite of the high speed of farmland reduction, Huzhou is still at the bottom of the ranking list. Such a phenomenon is closely related to the development of the city and is also consistent with its urbanization
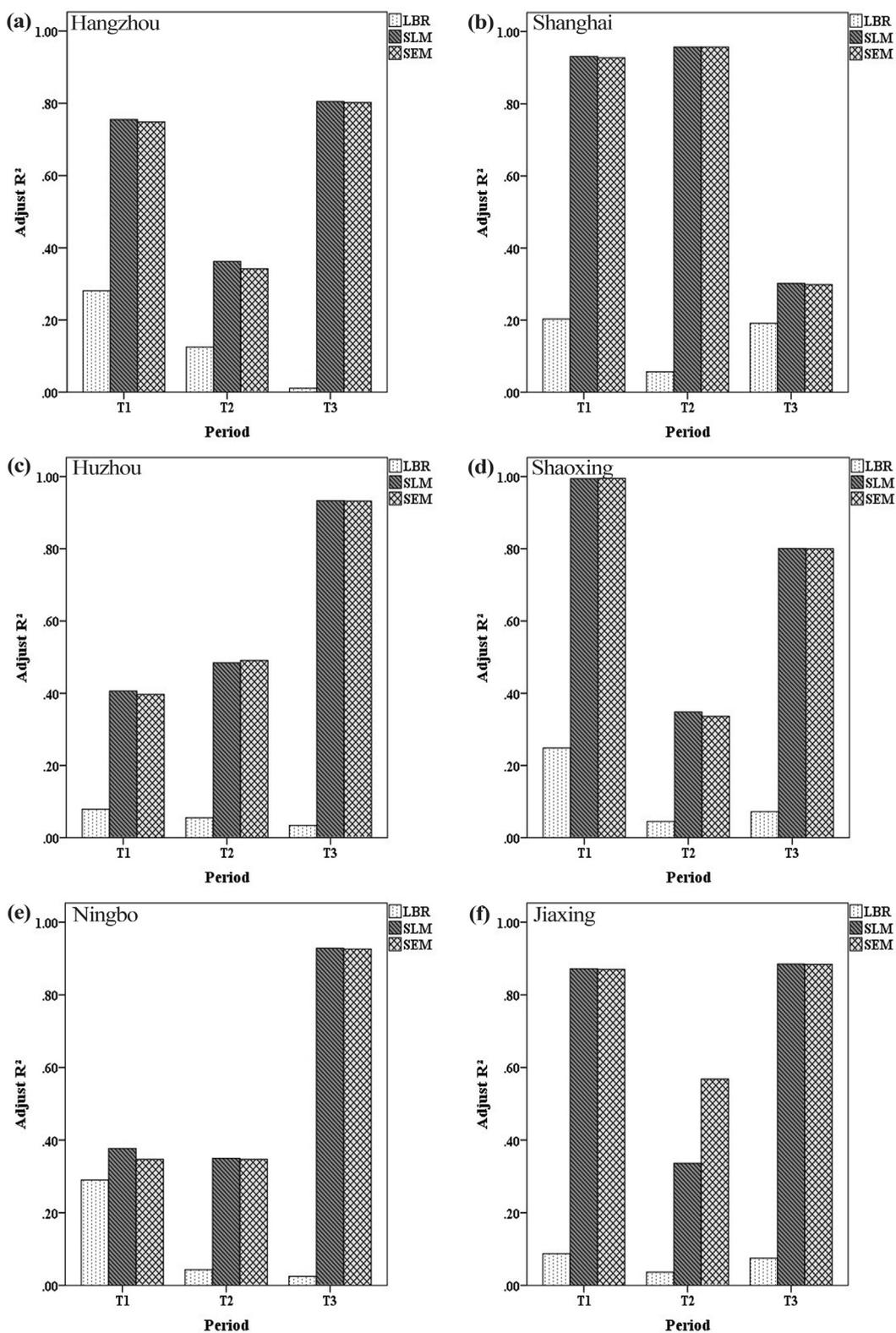
Fig. 6. Comparison of the adjusted R2 between the three models (T1: 1994–2003, T2: 2003–2009, T3: 2009–2015; BLR: binary logistic regression, SLM: spatial lag model, SEM: spatial error model).

characteristics in the acceleration phase.

It is also worth mentioning that the proportion of cultivated land in Shanghai was the highest among all the cities 1994, 2003, and 2009, which can be seen in Fig. 4. However, in 2015, the rapid farmland loss in Jiaxing (which also has a relatively high proportion of farmland, but

reduced slowly) resulted in it becoming the administrative area with the highest proportion of farmland. This statistical result reflects that Jiaxing is gradually undertaking the role of the main grain producer in the SHB area. In contrast, as the city possesses the lowest proportion of farmland, Hangzhou has experienced a drastic reduction in farmland.
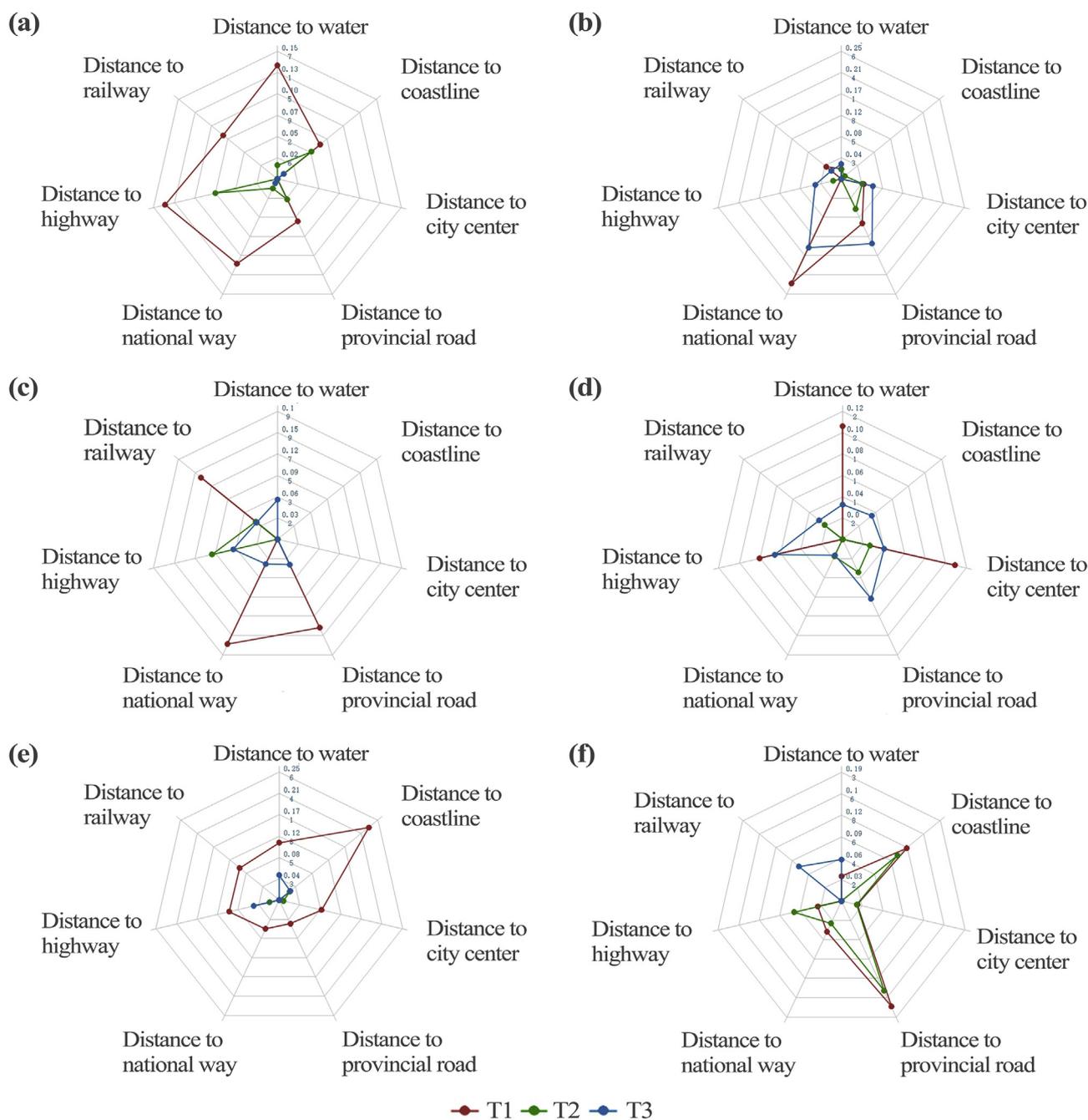
Fig. 7. The absolute values of the coefficients of the seven potential determinants according to BLR, SLM, and SEM (only those values passing the significance test are presented). T1: 1994–2003, T2: 2003–2009, T3: 2009–2015. (a) Hangzhou. (b) Shanghai. (c) Huzhou. (d) Shaoxing. (e) Ningbo. (f) Jiaxing.

As a result, this city held only 9% of the cultivated land in 2015, which may pose a threat to the agricultural industry in this area.

Except for the total area, the center and direction of cultivated land also migrated, which can be clearly seen by the characteristic values of the standard deviation ellipses. As exhibited in Fig. 5, the distribution of cultivated land in some cities (such as Huzhou) remained almost unchanged, while that was not the case for others. For Shanghai, the oblateness of the ellipse was reduced from 0.49 to 0.15 during T1 (1994–2003), reflecting an increased dispersion degree of farmland, and the spatial direction of farmland distribution was to the northeast in 1994 and 2009 and to the northwest in 2003 and 2015, which indicates a continuously changing trend. The weighted mean center moved from the west to the east during the study periods, which may be due to the farmland increase near the coastal areas or the farmland

decrease in the inland areas. Similar changes also occurred in Shaoxing. With regard to Jiaxing, the strengthened directionality of the distribution signified that the influencing factors shifted toward simplification in recent years, which is different from the diversification trend in Shanghai. Furthermore, as a typical example under some policies, the arable land center in Ningbo clearly shifted to the shoreline during the first period.

4.2. Results of the BLR models

The driving forces of the farmland change identified by the BLR models are presented in Table 2. For the six cities in the three intervals, AUC ROC ranges between 0.55 and 0.87, and adjusted R^2 reaches 0.01–0.29. This result suggests that only a few models, which were

mainly concentrated in T1, performed well enough in explaining the process of cultivated land change. Spatially, the models of Shanghai and Hangzhou city fitted better than the others. Aiming at these effective models, it can be found that the distance to water dominated in influencing most cities in T1, while in T2 and T3, multiple factors, including the distance to city center, distance to provincial road, distance to national road, and distance to railway, jointly exerted a significant impact.

Moreover, some determinants only played a key role in a particular city. For example, due to the establishment of the Land Reclamation Policy (LRP) in 2000, offshore areas were redeveloped into arable land, especially in Ningbo. The negative coefficient of −0.233 in T1 meant that a closer distance to the coastline resulted in a greater possibility of cultivated land change. Besides, the city center mainly had an effect on its surrounding cultivated land in Shanghai and Shaoxing.

4.3. Results of the two spatial regression models

As viewed from the perspective of adjusted R^2 in Table 3, more than 10 values exceed 0.7, and even the minimum value reaches 0.302, which denotes a good predictive ability and fitting degree for these spatial models. Higher values of adjusted R^2 imply that the driving factors in the research region are better explained by the spatial regression model than the logistic regression model. The coefficient of each factor reflects its influence over the farmland; for a negative value, the farther the distance from the factor, the smaller the probability that change occurred.

During the period of T1, it can be found that distance to water (D_{wt}) exhibited a strong effect in most cities, except for Hangzhou, while in T3, distance to roads (provincial road (D_{pr}), national road (D_{nr}), highway (D_{hw}), and railway (D_{rw})) gradually became dominant in these areas. Furthermore, the city center exhibited no appreciable effect during the three periods, especially in T3. Apart from the temporal differences, the spatial regression model focuses more on spatial diversities, which can be attributed to the various developmental modes in each city. For instance, the distance to main traffic roads was the most important driving force in Shanghai, while this influence was weaker in the other cities. It is because Shanghai possesses a more crowded road network than the other cities, which severely cuts down the area of cultivated land. Meanwhile, the spatial regression model also shows the remarkable impact of distance to coastline (D_{cl}) in Ningbo across T1 to T2, which is similar to the results of the logistic regression model.

5. Discussion

5.1. Response of cultivated land to urbanization

Urbanization is one of the principal characteristics and hot spot issues of regional coordinative development in modern China (Yuan et al., 2014). A common view is that urbanization is a diffusion process, which starts from the continuously growing urban centers that affect the remote rural villages in concentric circles (Bryant et al., 1982). The cities encompassed in our study area have also been found to demonstrate a similar trend. As the largest trade area in eastern China, the SHB area has a strong economy, thereby bringing about advanced urbanization. However, the intensive expansion of constructed impervious surfaces, spurred on by the rapid socio-economic development (Luo et al., 2017), has greatly affected the SHB area, and consequently resulted in large-scale farmland loss. It could be attributed to the fact that human settlement occupied more space on farming soils, since they were generally located in plains with better accessibility to cities or transportation routes (Pan and Zhao, 2007). The massive loss of cultivated land has inevitably led to food security crises and even high unemployment in non-urban areas (Xiao et al., 2013a,b).

Our research also proved that the megacity has a radiation effect upon its adjacent small- and medium-sized cities and towns under the process of urbanization (Chace and Walsh, 2006), which can be verified by Shanghai and Jiaxing. On the one hand, the rural population of Jiaxing flowed into Shanghai to seek job opportunities, aggravating the local farmland loss. On the other hand, the road network radiating from Shanghai also destroyed the arable land in the surrounding areas. A similar phenomenon has been observed in the Beijing-Tianjin-Hebei region (Tan et al., 2005) and Japan (Morikawa, 1990). It is also necessary to point out that some coastal cities (Shanghai, Ningbo, Jiaxing, Shaoxing, Hangzhou) exhibited analogous variations in farmland patterns (i.e., the area of cultivated land along the coastline increased to a certain extent) mainly due to the Land Reclamation Policy (LRP).

5.2. Comparison between BLR, SLM, and SEM

Reviewing the recent relevant studies (Su et al., 2014a,b,c; Garizi et al., 2012), it can be found that a single model (logistic regression/spatial regression) has usually been adopted to investigate the driving mechanisms of LULC change under urbanization. To detect and avoid the deficiency of a certain model, we used a combination of BLR, SLM, and SEM in this study. All three models are devised to characterize the association between dependent variable and multiple independent variables. However, due to the limit value (0/1) of the dependent variable, the results of BLR are more likely to verify whether the independent variable contributes to the occurrence of the event of interest (Hosmer and Lemeshow, 2000).

Compared with BLR, the spatial regression models reveal more about the lag or error of the influence on farmland in space. Similar changes were observed in adjacent areas, implying that notable spatial agglomeration and spatial diffusion exist in our research region. Therefore, the logistic regression model that covers the spatial effect will cause deviation of the estimated results (Baus et al., 2014), which can be confirmed by the low adjusted R^2 values (Fig. 6). In summary, spatial analysis, which serves as an efficient tool for quantitatively modeling cultivated land changes and offers an efficacious method for analyzing complex spatial patterns, is better suited to the SHB area.

Meanwhile, as Fig. 6 shows, the regression diagnostics also show that only three SEMs in the spatial analysis performed better than the SLM (T2 of Huzhou, T1 of Shaoxing, T2 of Jiaxing). Similar results were also obtained by Zhang et al. (2013). Models with a better fitting degree are mostly concentrated in the T3 period, while the poorer ones are concentrated in the T2 period, which can be ascribed to the temporal differences. Thus, the need for changing the time interval when characterizing the changes of arable land patterns should be stressed.

5.3. Driving force analysis

Through combining the results obtained by the different methods, all the potential driving factors we identified were found to play a role in the process of farmland reduction, varying with cities and periods. These differences appeared because of the diverse external environments and disparate soil conditions. Among the driving factors, the traffic network exerted the greatest influence on the farmland loss, and this influence varied with the road type (Qiu, 2009). According to Fig. 7, our research revealed that the distance to provincial road (D_{pr}) and national road (D_{nr}) influenced the cultivated land the most, followed by the distance to highway (D_{hw}), while railways had only a slight impact. In Shanghai, where the development of the economy brought about a great requirement for transportation, the LULC was severely impaired by the transportation routes (Su et al., 2014a,b,c).

River transportation was also important in the early stage. Our results suggested that distance to water (D_{wt}) had a significant negative effect on farmland during T1 in various areas. However, this impact declined with the reduction in waterway transport in T2 (Tables 2 and 3). With the demand for an improved living environment, many people have gradually tended to settle near to rivers and lakes. In our study

region, the districts near Hangzhou Bay and along the Qiantang River were always the most prosperous. Consequently, the water system became the main factor affecting the loss of cultivated land in recent years. In the Balçova Delta in Turkey, Bolca et al. (2007) explored the effect of the water on wetlands and marshes, obtaining similar conclusions.

The city centers were important in the early urbanization. After the most dramatic period of construction, not much cultivated land remained in the city centers, so the influence of this factor was weakened. In addition, the incredibly high prices and crowded traffic also hindered people from settling in the downtown areas. As for the coastline, it only showed an evident impact on Ningbo during T1 in our research. What is more, under the implementation of the LRP, the effect of natural physical and chemical processes was obscured. In Portugal, Freire et al. (2009) reported that the presence of artificial surfaces homogeneously decreased with the distance to the coastline. It would be meaningful to further evaluate the urbanization pressure and change rates under the framework of the "coastal carrying capacity" (Carver and Mallet, 1990), so as to study the coastal sustainability for the SHB area.

5.4. Implications and limitations

Over the past 20 years, the rapid urbanization of the SHB area has led to a great conversion of LULC types. To boost economic development, the government has sold a great quantity of high-quality agricultural land to real estate developers, which has caused the cultivated land to decrease in area and fragment. The Food and Agriculture Organization (FAO) of the United Nations proclaimed that the per capita arable land in Zhejiang province is lower than the precautious line (Zhang et al., 2014). Hence, the government should formulate a long-term strategy to strengthen the theoretical research on the protection of cultivated land and enhance the constitution, implementation, and supervision of the protection policy. Not only that, in view of the particular geographical location of coastal areas, the one-size-fits-all approach cannot apply in the SHB area. Local government is responsible for incorporating the national protection policy into local land-use practice and taking the spatial spill-over effect into account (Su et al., 2017). Based on the SLM and SEM, we know that people prefer to dwell near to wide roads (provincial roads and national roads) rather than in downtown areas. Considering the impact of transportation routes, the relevant departments should rationally design the road network in urban planning, to avoid over-segmentation of the farmland. Meanwhile, the protection of the farmland near to the river system of the Yangtze Delta also needs further research and vigorous land-use planning.

Despite the use of the novel method combining BLR, SLM, and SEM in this study, several limitations exists. Firstly, we only selected seven proximate factors as potential driving forces to conduct the investigation. Actually, for most LULC patterns, the behavioral and structural factors are usually divided into four categories: proximity, physical factors, neighborhood, and socio-economic determinants (Liao and Wei, 2014). Factors such as climate, land price, inefficient cultivation, and decreasing numbers of farmers should also be considered in future investigations. Secondly, this study was carried at the municipal scale, and such generalized research may mask the spatial distinctions of smaller regions (e.g., county, town, etc.). Some researchers have proposed that any modeling attempt at a regional level should integrate a thorough analysis of the effects of the spatial scale (Kok and Veldkamp, 2001; Liu et al., 2016). Thirdly, given the poor resolution of the TM imagery, the accuracy of the farmland distribution map is limited. Finally, we did not consider those transportation routes under construction in each period, bringing a slight roughness to our results. A deeper understanding could be achieved by taking these points into consideration in future studies.

6. Conclusion

In this study, we undertook a comprehensive application of BLR, SLM, and SEM in exploring the spatially varying determinants of farmland loss under urbanization at an administrative scale. China has witnessed booming urbanization after the implementation of the "reform and opening-up" policy, which has directly led to cultivated land shrinkage and indirectly caused food shortage. The urbanization of the SHB area, the biggest urban agglomeration in the eastern coast of China, has been not only rapid, but also shows obvious sprawl and diversity in space. The results of this study showed that Shanghai went through the most dramatic decline in farmland during the three periods (1994–2003, 2003–2009, 2009–2015), followed by Hangzhou. In addition, serious farmland loss initially appeared around the city centers and then spread to the suburbs. The regression analysis of the potential driving forces and farmland change indicated that the farmland near to transportation routes faced a higher risk of conversion in most cities and periods, while the water and coastline played a role only in certain regions and times (e.g., water played a role in Shaoxing, Jiaxing, and Huzhou during T1 and T3, and coastline effected Ningbo during T1). Therefore, road planning and regional differences are the primary aspects that the government should take into consideration when formulating urban development policies.

Our study also hinted that the common BLR model failed to reflect the real dynamics of farmland loss under the accelerating urbanization in the SHB area, while the spatial regression models displayed a better performance. Such findings highlight the spatial non-stationarity in large research areas. Finally, the limitations existing in this study should not be neglected: the data sources with a coarse resolution, the insufficiency of the selected driving factors, and the generalized scale of the municipal administrative district. Based on these conclusions, we propose that further studies on farmland loss in response to urbanization should be conducted at a smaller scale, and the scale effect should be taken into consideration. Moreover, the impacts of farmland pattern changes on the eco-society resource allocation, the spatial spill-over and diffusion in large cities, and the according policy implications should also be addressed.

Acknowledgements

References

Anselin, L., 1995. Local indicators of spatial association—LISA. Geogr. Anal. 27 (2), 93–115.

Baus, P., Kováč, U., Pauditšová, E., Kohutková, I., Komorník, J., 2014. Identification of interconnections between landscape pattern and urban dynamics—case study bratislava, slovakia. Ecol. Indic. 42, 104–111.

Bolca, M., Turkyilmaz, B., Kurucu, Y., Altinbas, U., Esetlili, M.T., Gulgun, B., 2007. Determination of impact of urbanization on agricultural land and wetland land use in Balçovas' delta by remote sensing and GIS technique. Environ. Monit. Assess. 131 (1–3), 409–419.

Bryant, C.R., Russwurm, L.J., Mclellan, A.G., 1982. The City's Countryside – Land and its Management in the Rural-urban Fringe. Longman, New York.

Carver, C.E.A., Mallet, A.L., 1990. Estimating the carrying capacity of a coastal inlet for mussel culture. Aquaculture 88 (1), 39–53.

Chace, J.F., Walsh, J.J., 2006. Urban effects on native avifauna: a review. Landsc. Urban Plan. 74 (1), 46–69.

Chaudhuri, G., Mishra, N.B., 2016. Spatio-temporal dynamics of land cover and land surface temperature in Ganges-Brahmaputra delta: a comparative analysis between India and Bangladesh. Appl. Geogr. 68, 68–83.

Durina, Nagasawa, R., Patanakano, B., 2013. Urbanization and its influences on the suburban landscape changes in Bangkok metropolitan region, Thailand. J. Jpn. Agric. Syst. Soc. 29, 29–39.

Eryando, T., Susanna, D., Pratiwi, D., Nugraha, F., 2012. Standard Deviational Ellipse (SDE) models for malaria surveillance, case study: Sukabumi district-Indonesia, in

2012. Malar. J. 11 (1), 1–2.

Fang, C., Li, G., Wang, S., 2016. Changing and differentiated urban landscape in China: spatio-temporal patterns and driving forces. Environ. Sci. Technol. 50 (5), 2217–2227.

Freire, S., Santos, T., Tenedório, J.A., 2009. Recent urbanization and land use/land cover change in Portugal — the influence of coastline and coastal urban centers. J. Coast. Res. 25 (1), 1499–1503.

Garizi, A.Z., Sheikh, V., Sadoddin, A., Mahiny, A.S., 2012. Modeling the spatial pattern of land-cover change, using logistic regression (Case study: Chehlchay watershed, Golestan province). J. Oral Maxillofac. Surg. 63 (8Suppl1), 93–94.

Gong, J.X., 2002. Clarifying the standard deviational ellipse. Geogr. Anal. 34 (2), 155–167.

Haygarth, Ritz, K., 2009. The future of soils and land use in the UK: soil systems for the provision of land-based ecosystem services. Land Use Pol. 26 (9), 187–197.

Hosmer, D.W., Lemeshow, S., 2000. Applied Logistic Regression. J. Wiley, New Jersey.

Hu, J., Zhang, Y., 2013. Seasonal change of land-use/land-cover (LULC) detection using MODIS data in rapid urbanization regions: a case study of the Pearl River Delta Region (China). IEEE J. Sel. Top. Appl. Earth Observ. Remote Sens. 6 (4), 1913–1920.

Huang, J., Zhu, L., Deng, X., 2005. Cultivated land changes in China: the impacts of urbanization and industrialization. Remote Sens. Model. Ecosyst. Sustain. II. 5884, 135–149.

Jiang, L., Ji, M., 2011. Spatial effect in the analysis of technological progress and energy efficiency in China — An empirical study based on a spatial econometric model. Poster session presentation at the meeting of the IEEE International Conference on Geoinformatics, Shanghai, China.

Kacprzak, E., Maćkiewicz, B., 2013. Farmland conversion and changes in the land- use pattern in the poznaŃ agglomeration over the years 2000–2009. Quaestiones Geographicae 32 (4), 91–102.

Kent, J., Leitner, M., 2007. Efficacy of standard deviational ellipses in the application of criminal geographic profiling. J. Investig. Psychol. Offender Profiling 4 (3), 147–165.

Kok, K., Veldkamp, A., 2001. Evaluating impact of spatial scales on land use pattern analysis in Central America. Agric. Ecosyst. Environ. 85 (1–3), 205–221.

Lambin, E.F., Meyfroidt, P., 2010. Land use transitions: socio-ecological feedback versus socio-economic change. Land Use Pol. 27 (2), 108–118.

Lefever, D.W., 1926. Measuring geographic concentration by means of the standard de- viational ellipse. Am. J. Sociol. 32 (1), 88–94.

Li, X., Zhou, W., Ouyang, Z., 2013. Forty years of urban expansion in Beijing: what is the relative importance of physical, socioeconomic, and neighborhood factors? Appl. Geogr. 38 (1), 1–10.

Liao, F.H.F., Wei, Y.H.D., 2014. Modeling determinants of urban growth in Dongguan, China: a spatial logistic approach. Stoch. Environ. Res. Risk Assess. 28 (4), 801–816.

Luo, K., Hu, X., He, Q., Wu, Z., Cheng, H., Hu, Z., Mazumder, A., 2017. Impacts of rapid urbanization on the water quality and macroinvertebrate communities of streams: A case study in Liangjiang New Area. China. Sci. Total Environ. 621 (10), 1601–1614.

Liu, Y., Wei, X., Li, P., Li, Q., 2016. Sensitivity of correlation structure of class- and landscape-level metrics in three diverse regions. Ecol. Indic. 64, 9–19.

Mason, S.J., Graham, N.E., 2002. Areas beneath the relative operating characteristics (ROC) and relative operating levels (ROL) curves: statistical significance and inter- pretation. Q. J. R. Meteorol. Soc. 128 (584), 2145–2166.

Menard, S., 2012a. Applied logistic regression analysis. Technometrics 38 (2), 192.

Menard, S., 2012b. Six approaches to calculating standardized logistic regression coeffi- cients. Am. Stat. 58 (3), 218–223.

Morikawa, H., 1990. The relationship between wider-area municipal spheres and regional urban systems in Japan. Geogr. Rev. Jpn. 63, 356–377.

Oruonye, E.D., 2014. An assessment of the impact of road construction on land use pattern in urban centres in Nigeria, a case study of Jalingo LGA, Taraba State Nigeria. Mediterr. J. Soc. Sci. 5 (10), 82–88.

Osawa, T., Kohyama, K., Mitsuhashi, H., 2016. Multiple factors drive regional agricultural abandonment. Sci. Total Environ. 542 (Pt A), 478–483.

Pan, X.Z., Zhao, Q.G., 2007. Measurement of urbanization process and the paddy soil loss in Yixing city, China between 1949 and 2000. Catena 69 (1), 65–73.

Pazúr, R., Lieskovský, J., Feranec, J., Oťaheľ, J., 2014. Spatial determinants of aban- donment of large-scale arable lands and managed grasslands in Slovakia during the periods of post-socialist transition and European union accession. Appl. Geogr. 54, 118–128.

Qiu, M., 2009. Evaluating the temporal and spatial urban expansion patterns of

Guangzhou from 1979 to 2003 by remote sensing and GIS methods. Int. J. Geogr. Inf. Sci. 23 (11), 1371–1388.

Lee, S., 2005. Application of logistic regression model and its validation for landslide susceptibility mapping using gis and remote sensing data. Int. J. Remote Sens. 26 (7), 1477–1491.

Shanghai Statistical Yearbook, 2016. Beijing: China Statistics Press (in Chinese).

Shu, B.R., Zhang, H.H., Li, Y.L., Qi, Y., Chen, L.H., 2014. Spatiotemporal variation ana- lysis of driving forces of urban land spatial expansion using logistic regression: a case study of port towns in Taicang City, China. Habitat Int. 43 (4), 181–190.

Su, S., Li, D., Hu, Y., Xiao, R., Zhang, Y., 2014a. Spatially non-stationary response of ecosystem service value changes to urbanization in Shanghai, China. Ecol. Indic. 45 (5), 332–339.

Su, S., Liu, Z., Xu, Y., Li, J., Pi, J., Weng, M., 2017. China's megaregion policy: perfor- mance evaluation framework, empirical findings and implications for spatial poly- centric governance. Land Use Pol. 63, 1–19.

Su, S., Ma, X., Xiao, R., 2014b. Agricultural landscape pattern changes in response to urbanization at ecoregional scale. Ecol. Indic. 40, 10–18.

Su, S., Xiao, R., Zhang, Y., 2012. Multi-scale analysis of spatially varying relationships between agricultural landscape patterns and urbanization using geographically weighted regression. Appl. Geogr. 32 (2), 360–375.

Su, S., Liu, Z., Li, D., Hu, Y., 2014c. Impacts of transportation routes on landscape di- versity: a comparison of different route types and their combined effects. Environ. Manage. 53 (3), 636–647.

Su, S., Xiao, R., Mi, X., Xu, X., Zhang, Z., Wu, J., 2013. Spatial determinants of hazardous chemicals in surface water of Qiantang River, China. Ecol. Indic. 24 (24), 375–381.

Tan, M., Li, X., Xie, H., Lu, C., 2005. Urban land expansion and arable land loss in China—a case study of Beijing–Tianjin–Hebei region. Land Use Pol. 22 (3), 187–196.

Tayyebi, A., Pijanowski, B.C., 2014. Modeling multiple land use changes using ANN, CART and MARS: comparing tradeoffs in goodness of fit and explanatory power of data mining tools. Int. J. Appl. Earth Obs. Geoinf. 28 (28), 102–116.

Wang, B., Shi, W., Miao, Z., 2015. Confidence analysis of standard deviational ellipse and its extension into higher dimensional Euclidean space. PLoS One 10 (3), e0118537.

Wu, W., Zhao, S., Zhu, C., Jiang, J., 2015. A comparative study of urban expansion in Beijing, Tianjin and Shijiazhuang over the past three decades. Landsc. Urban Plan. 134, 93–106.

Wu, X., Liu, C., Wu, G., 2018. Spatial-temporal analysis and stability investigation of coastline changes: a case study in Shenzhen, China. IEEE J. Sel. Top. Appl. Earth Observ. Remote Sens. 11 (1), 45–56.

Xiao, R., Su, S., Ghadouani, A., Wu, J., 2013a. Spatial analysis of phytoplankton patterns in relation to environmental factors across the southern Taihu basin, China. Stoch. Environ. Res. Risk Assess. 27 (6), 1347–1357.

Xiao, R., Su, S., Mai, G., Zhang, Z., Yang, C., 2015. Quantifying determinants of cash crop expansion and their relative effects using logistic regression modeling and variance partitioning. Int. J. Appl. Earth Obs. Geoinf. 34 (1), 258–263.

Xiao, R., Su, S., Zhang, Z., Qi, J., Jiang, D., Wu, J., 2013b. Dynamics of soil sealing and soil landscape patterns under rapid urbanization. Catena 109 (10), 1–12.

Yan, X., Cai, Y.L., 2015. Multi-scale anthropogenic driving forces of Karst rocky deserti- fication in Southwest China. Land Degrad. Dev. 26 (2), 193–200.

Yuan, Y.Q., Jin, M.Z., Ren, J.F., Hu, M.M., Ren, P.Y., 2014. The dynamic coordinated development of a regional environment-tourism-economy system: a case study from western Hunan Province, China. Sustainability 6 (8), 5231–5251.

Zhang, Q., Wallace, J., Deng, X., Seto, K.C., 2014. Central versus local states: which matters more in affecting China's urban growth? Land Use Pol. 38 (38), 487–496.

Zhang, X., Chen, J., Tan, M., Sun, Y., 2007. Assessing the impact of urban sprawl on soil resources of Nanjing city using satellite images and digital soil databases. Catena 69 (1), 16–30.

Zhang, Z., Su, S., Xiao, R., Jiang, D., Wu, J., 2013. Identifying determinants of urban growth from a multi-scale perspective: a case study of the urban agglomeration around Hangzhou Bay, China. Appl. Geogr. 45 (45), 193–202.

Zhejiang Statistical Yearbook, 2016. Beijing: China Statistics Press (in Chinese).

Zhou, Y., Xing, B., Ju, W., 2017. Assessing the impact of urban sprawl on net primary productivity of terrestrial ecosystems using a process-based model—a case study in Nanjing, China. IEEE J. Sel. Top. Appl. Earth Observ. Remote Sens. 8 (5), 2318–2331.

Zhou, Z.X., Li, M.T., 2017. Spatial-temporal change in urban agricultural land use effi- ciency from the perspective of agricultural multi-functionality: a case study of the Xi'an metropolitan zone. J. Geogr. Sci. 27 (12), 1499–1520.